



1

2 **Dependence between the Photochemical Age of Light Aromatic Hydrocarbons and the**
3 **Carbon Isotope Ratios of Atmospheric Nitrophenols**

4 **Marina Saccon¹, Anna Kornilova¹, Lin Huang², Jochen Rudolph¹**

5 Affiliation:

6 1. Centre for Atmospheric Chemistry

7 York University

8 4700 Keele St.

9 Toronto, ON.

10 M3J 1P3

11

12 2. Climate Research Division

13 Atmospheric Science & Technology Directorate

14 STB, Environment & Climate Change Canada

15 4905 Dufferin St.

16 Toronto, ON.

17 M3H 5T4

18

19

20

21

22

23

24

25

26

27

28

29

30

31

32

33

34

35

36

37



1 Abstract

2 Concepts were developed to establish relationships between the stable carbon isotope
3 ratios of nitrophenols in the atmosphere and photochemical processing of their precursors, light
4 aromatic volatile organic compounds. The concepts are based on the assumption that
5 nitrophenols are formed dominantly from the photo-oxidation of aromatic VOC. A mass balance
6 model as well as various scenarios based on the proposed mechanism of nitrophenol formation
7 were formulated and applied to derive the time integrated exposure of the precursors to
8 processing by OH-radicals ($\int[\text{OH}]dt$) from ambient observations taken between 2009 and 2012 in
9 Toronto, Canada. The mechanistic model included the possibility of isotopic fractionation during
10 intermediate steps, rather than during the initial reaction step alone. This model included
11 knowledge of kinetic isotope effects of the precursor VOC with the hydroxyl radical and their
12 respective rate constants, as well as isotope ratio source signatures. While many of these values
13 are known, there were some, such as the kinetic isotope effects of reactions of the intermediate
14 compounds, which were unknown. These values were predicted based on basic principles and
15 published laboratory measurements of normal kinetic carbon isotope effects and were applied to
16 the mechanistic models. Due to uncertainty of the estimates based on general principles three
17 scenarios were used with different values for isotope effect that were not known from laboratory
18 studies. Comparison of the dependence between nitrophenol carbon isotope ratios and $\int[\text{OH}]dt$
19 with published results of laboratory studies and ambient observations was used to narrow the
20 range of plausible scenarios of the mechanistic model and to eliminate the mass balance based
21 model as useful formulation of a the dependence between nitrophenol carbon isotope ratios and
22 $\int[\text{OH}]dt$.

23



1 **1 Introduction**

2 Secondary organic aerosols (SOA) in the atmosphere, formed from the photo-oxidation
3 of both anthropogenic and biogenic volatile organic compounds (VOC) are poorly understood.
4 Products formed from these reactions are only partly known and beyond the composition of
5 SOA, little is also known about its atmospheric processing. It has been proposed that the use of
6 concentration measurements in conjunction with stable carbon isotope ratio measurements can
7 be used to gain insight into this topic (Goldstein and Shaw, 2003; Rudolph, 2007; Gensch et al.,
8 2014). The compounds of interest in this study are nitrophenols, which have been proposed to be
9 formed specifically from the gas phase photo-oxidation of aromatic VOC (Forstner et al., 1997;
10 Atkinson, 2000; Jang and Kamens, 2001; Hamilton et al., 2005; Sato et al., 2007). Once toluene,
11 for example, is emitted from its anthropogenic sources, it is expected to react according to the
12 proposed reaction mechanism (Forstner et al., 1997) to produce methylnitrophenols (Fig. 1). By
13 being formed specifically from identified reactions, the stable carbon isotope ratio of the product
14 can be linked back to the precursor and its source. Additionally, methylnitrophenols were found
15 to have an average isotope ratio that is close to the isotope ratio of the sum of all products from
16 mass balance observations in the laboratory (Irei et al., 2011). The aqueous phase production of
17 nitrophenols, specifically 4-nitrophenol, has also been proposed through a reaction pathway with
18 the NO₃ radical (Hermann et al., 1995; Harrison et al., 2005). This pathway has been proposed to
19 be a quite significant source of 4-nitrophenol in the presence of clouds with high liquid water
20 content but has been modelled to contribute less than 2 % when the liquid water content is low
21 (Harrison et al., 2005). Ambient measurements in the Toronto area (Saccon et al., 2015) indicate
22 that nitrophenols are dominantly formed from secondary processes due to their depleted stable
23 carbon isotope ratio.



1 The carbon isotope ratio of a species, which will be referred to as the delta value ($\delta^{13}\text{C}$),
2 is defined using Eq. 1, where $(^{13}\text{C}/^{12}\text{C})_{\text{V-PDB}}$ is the internationally accepted Vienna-Peedee
3 Belemnite (V-PDB) value of 0.0112372. Since differences in isotope ratios between species are
4 small, delta values are expressed in per mille notation. Limited studies using the isotope ratio of
5 atmospheric trace components, including several aromatic VOC and nitrophenols in SOA, have
6 been applied to differentiate between sources and to trace components back to the precursor,
7 respectively (Moukhtar et al., 2011; Kornilova et al., 2013; Saccon et al., 2013). The concept to
8 derive information on photochemical processing of trace constituents from isotope ratios is based
9 on the kinetic isotopic effect (KIE) which describes the dependence of the rate constant of a
10 reaction on the atomic mass of isotopologues. In this work, the KIE will be referred to as ε (Eq.
11 2), where k_{12} and k_{13} are the rate constants for the ^{12}C only and ^{13}C containing species,
12 respectively. Normal KIE, that is when ε is larger than one, is exhibited when a compound reacts
13 in the atmosphere and becomes enriched in heavier isotopes, for example the ^{13}C isotopes. Like
14 delta values, ε is also expressed in per mille notation.

$$\delta^{13}\text{C} = \frac{(^{13}\text{C}/^{12}\text{C})_{\text{sample}} - (^{13}\text{C}/^{12}\text{C})_{\text{V-PDB}}}{(^{13}\text{C}/^{12}\text{C})_{\text{V-PDB}}} \times 1000\text{‰} \quad \text{Eq. 1}$$

$$\varepsilon = \frac{k_{12} - k_{13}}{k_{13}} \times 1000\text{‰} \quad \text{Eq. 2}$$

15

16 The concentration of a species in the atmosphere will, among other factors, depend on its
17 reactivity and the time that it has been exposed to reactants. For many VOC and semi-volatile
18 organic compounds (SVOC) the most important reactant is the OH radical, and the time
19 integrated OH radical concentration is often referred to as the photochemical age (PCA). The
20 combination of laboratory experiments and ambient measurements can allow the determination



1 of the PCA of a specific component in SOA. The PCA of a species has been previously used to
2 quantify the extent of processing of a precursor using the hydrocarbon clock by using mixing
3 ratios of VOC (Parrish et al., 1992; Jobson et al., 1998, Jobson et al., 1999; Kleinman et al.,
4 2003; Parrish et al., 2007). A more recently developed method uses the isotope ratio of an
5 ambient species, the KIE and the isotope ratio source signature to determine the PCA and is
6 referred to as the isotope hydrocarbon clock (Rudolph and Czuba, 2000; Rudolph et al., 2003;
7 Thompson, 2003; Stein and Rudolph, 2007; Kornilova, 2012, Kornilova et al., 2016). The PCA
8 of a species can be calculated using Eq. 3, where $\delta^{13}\text{C}_{\text{pre}}$ is the isotope ratio of the measured
9 ambient precursor, $\delta^{13}\text{C}_0$ is the isotope ratio of the emissions, and $\int[\text{OH}]dt$ is the time integrated
10 OH concentration. However, it has been shown that the concept of ascribing a photochemical age
11 to an air mass (Parrish et al., 1992) is only meaning full if all individual air parcels that
12 contribute to the observed VOC mixing ratios have been subject to an identical extent of
13 processing. In case of mixing air masses with VOC having been subject to different extent of
14 processing the concept of a photochemical age of an air mass has to be replaced by the concept
15 of a photochemical age of an individual VOC (Kornilova et al., 2016). It has been shown by
16 Rudolph and Czuba (2000) that VOC carbon isotope ratio measurements can be used to
17 determine the concentration weighted average of the photochemical age of individual VOC
18 provided the variability of the carbon isotope ratio of emissions is small compared to the change
19 in carbon isotope ratio resulting from atmospheric removal reactions.

20 The carbon isotope ratio of the emissions of many important anthropogenic VOC
21 precursors has been previously measured and their uncertainty typically is below 1 ‰
22 (Czapiewski et al., 2002; Rudolph et al., 2002; Rudolph, 2007, Gensch et al, 2014). The change
23 in VOC mixing ratios due to reaction with OH-radicals can be described by Eq. 4, where χ_{amb} and



1 χ_0 are the mixing ratios of the ambient precursor and the mixing ratio that would be observed in
2 the absence of reaction with OH-radicals, respectively. Consequently a combination of carbon
3 isotope ratio measurements allows separating between the impact of atmospheric reactions and
4 changes in source strength or atmospheric mixing and dilution.

$$\delta^{13}C_{pre} = \delta^{13}C_0 + k_{12}\varepsilon \int [OH]dt \quad \text{Eq. 3}$$

$$\chi_{amb} = \chi_0 \exp(-k_{12} \int [OH]dt) \quad \text{Eq. 4}$$

5

6 Comparison of the difference between χ_0 and χ_{amb} with the ambient concentrations of the
7 products of the photochemical reactions of VOC will provide insight into the yield of the
8 secondary pollutants from the reaction. However, in the case of mixing air masses containing
9 VOC with different photochemical ages, Eq. 4 will underestimate χ_0 and only provides
10 information of the minimum contribution from emissions, although Eq. 3 still is a very good
11 approximation for the concentration weighted average $\int [OH]dt$ of the precursor VOC (Rudolph
12 and Czuba, 2000). Consequently yield estimates derived from combining results derived from
13 Eq. 3 and 4 with measured ambient concentrations of reaction products will be an upper limit. In
14 principle this limitation can be avoided by using the carbon isotope ratio of the reaction product
15 to derive $\int [OH]dt$ since the average of $\int [OH]dt$ derived from carbon isotope ratios of the reaction
16 products will be weighted according to the concentration of the products, which will accumulate
17 as result of the photochemical reaction of the precursor. However, the relation between the
18 carbon isotope ratio of the reaction product and the extent of photochemical processing is more
19 complex than the simple relation between the carbon isotope ratio of the precursor and $\int [OH]dt$
20 described by Eq. 3.



1 The reported isotope ratio measurements of nitrophenols in the solid and the gas phase by
2 Saccon et al. (2015) have shown that, although the average isotope ratios are consistent with
3 laboratory studies, a significant number of delta values are approximately 2 ‰ to 3 ‰ lower
4 than predicted from mass balance. This difference cannot be explained by the uncertainty of the
5 carbon isotope ratios of precursor emission or measurements error. However, a simple mass
6 balance only considers the KIE for the first step of the reaction mechanism, shown in Fig. 1 and
7 it must be accepted that further fractionation can occur in reaction steps following the initial
8 reaction of the aromatic VOC with the OH-radical. In this work, we will present mechanisms
9 based on formation and removal of nitrophenols from the atmosphere that describe the
10 dependence between photochemical processing of light aromatic hydrocarbons and the carbon
11 isotope ratio of nitrophenols, which are products of atmospheric reactions of light aromatic
12 hydrocarbons. The mechanisms will be discussed using the carbon isotope ratios of nitrophenols
13 published by Saccon et al. (2015) and the laboratory studies published by Irei et al. (2015).

14 **2 Materials and Method**

15 The experimental method used in this work is described in detail by Saccon et al. (2013),
16 which is based on methods developed by Moukhtar et al. (2011) and Irei et al. (2013). The
17 results of the isotope ratio measurements have been presented by Saccon et al. (2015) and we
18 therefore will only briefly describe the experimental procedure. Sample collection was done at
19 York University in Toronto, Canada using 20.32 cm x 25.4 cm quartz fiber filters (Pallflex®
20 Tissuquartz™ filters – 2500 QAT – PallGelman Sciences) on high volume air samplers (TE-
21 6001 from Tisch Environmental Inc.) equipped with PM2.5 heads. Uncoated quartz filters were
22 used to collect particulate matter (PM) alone, with an average sampling time of one to three days,



1 and filters coated with XAD-4TM resin were used for the collection of gas phase and PM, with an
2 average sampling time of one day. Filter samples were collected between March 2009 and
3 August 2012. The analysis of the filters included extraction in acetonitrile, and HPLC separation
4 and solid phase extraction were used as sample clean-up steps. Concentration measurements
5 were done using a HP 5890 GC equipped with a HP 5972 mass spectrometer; isotope ratio
6 measurements were done using a Micromass Isoprime IRMS (Isomass Scientific, Inc.). Method
7 performance characteristics are given in Saccon et al. (2013) and Saccon et al. (2015).

8 **3 Determination of PCA**

9 Laboratory experiments studying the carbon isotope ratios of secondary particulate
10 organic matter (POM) formed by the gas phase oxidation of toluene showed that the $\delta^{13}\text{C}$ value
11 of total secondary POM can be approximated by mass balance (Irei et al., 2006, 2011). However,
12 compound specific measurements also indicate that in some cases detailed mechanistic
13 considerations are required to explain the observed $\delta^{13}\text{C}$ values of secondary phenols that are
14 lower than expected from mass balance alone (Irei et al., 2015).

15 **3.1. PCA from Mass Balance**

16 Mass balance calculations allow a straightforward determination of the dependence
17 between the $\delta^{13}\text{C}$ of the total of secondary POM and the PCA. This requires the assumption that
18 in the atmosphere the carbon isotope ratio of the gas phase reaction products is identical to the
19 carbon isotope ratio of secondary POM as observed in laboratory studies (Irei et al., 2006, 2011).
20 Furthermore, for compound specific isotope ratio measurements it also has to be assumed that
21 the isotope ratio of the individual products is representative for the carbon isotope ratio of all
22 secondary POM. In this case the dependence between PCA of the precursors and the product



1 isotope ratio (Eq. 5) can be derived from Eq. 3 and Eq. 4. Here, k_{OH} is the averaged rate constant
2 of all isotopomers of the precursor reacting with OH and for practical purposes, is equal to k_{12} .

$$\delta^{13}C_{prod} = \frac{\delta^{13}C_o - \exp(-k_{OH} \int [OH] dt)(\delta^{13}C_o + k_{12} \epsilon \int [OH] dt)}{1 - \exp(-k_{OH} \int [OH] dt)} \quad \text{Eq. 5}$$

3
4 It should be noted that, similar to the conventional hydrocarbon clock, in the case of mixing of
5 air masses with different PCA, the PCA from Eq. 5 is a combination of the PCA of the individual
6 air masses, which is not always easy to interpret. Equation 5 also neglects possible isotope
7 fractionation resulting from loss of secondary POM. The values for rate constants, isotope ratio
8 of precursor VOC emissions and kinetic isotope effects used are listed in Table 1.

9

10 **3.2. PCA from detailed mechanistic concepts**

11 The presently known reaction sequence resulting in the formation of nitrophenols from
12 oxidation of toluene shown in Fig. 1 does not include details of the various branching reactions
13 and alternate pathways resulting in other products or isotope fractionation due to loss reactions of
14 secondary POM. While in many cases branching ratios are known, there is little direct
15 knowledge on isotope fractionation resulting from branching reactions. Nevertheless, isotope
16 effects for specific pathways can be estimated from the type of reaction and known principles of
17 isotope fractionation. For example, after formation of the cresol intermediate (Fig. 1), an OH
18 radical is added to the ring 92 % of the time (Atkinson et al., 1980) while reaction at the phenolic
19 OH group, which is expected to result in formation of nitrophenols, occurs with 8% probability.
20 The reaction of the phenolic OH group is expected to result in negligible carbon isotope fraction



1 since it is a secondary isotope effect, while the OH radical addition will have a carbon isotope
2 effect similar to that of other OH addition reactions to aromatic rings. Similarly, the main gas
3 phase loss process of nitrophenols is expected to be through reaction with the OH radical,
4 occurring through an OH addition to the ring greater than 80 % of the time (Bejan et al., 2007)
5 and since an OH radical is being added to the ring, fractionation typical for reaction at the
6 aromatic ring is expected to occur for 80% of the loss reactions.

7 Another complication is the distribution between gas phase and PM. It was assumed that
8 there are no chemical losses when the nitrophenols partition into PM, and that there is
9 equilibrium between the gas and particle phases. Since phase distribution processes typically
10 have very small isotope effects, partitioning between gas phase and PM is expected to have only
11 a marginal impact on the isotope ratio. This is consistent with the findings of Saccon et al.
12 (2015). However, partitioning will influence the loss rate for SVOC since it is assumed that there
13 is little to no chemical loss in the PM phase. Furthermore, uncertainty in phase partitioning will
14 only result in minor uncertainties of the photochemical nitrophenol loss rate since it has been
15 reported that only approximately 20 % of the nitrophenols partition into the particle phase
16 (Saccon et al., 2013, 2015).

17 There are also some reaction rate constants which for which no laboratory measurements
18 are available. The rate constant for 3-methyl-4-nitrophenol was estimated based on the position
19 of its substituents on the aromatic ring relative to other isomers that have known rate constants,
20 such as 3-methyl-2-nitrophenol and 4-methyl-2-nitrophenol. For 2,6-dimethyl-4-nitrophenol it
21 was assumed that loss reactions due to addition of the OH radical to the aromatic ring are
22 negligible since the nitro and hydroxyl substituents both direct reactions to positions that already
23 are occupied by other substituents and that reaction at positions 3 or 5 is unlikely to occur. It



1 should be noted that reaction at the phenolic OH-group of 2,6-dimethyl-4-nitrophenol will not
 2 impact the carbon isotope ratio since this secondary carbon isotope effect will be negligible,
 3 independent of the rate of this reaction. There is no information available that would allow
 4 estimating the rate of exchange of nitrophenols between gas phase and PM. It was assumed that
 5 phase partitioning is fast compared to gas phase reactions. There are indications that in some
 6 cases exchange between gas phase and PM is slower than formation or loss reactions of SVOC in
 7 the gas phase (Saccon et al., 2015), but the reported average of the difference in carbon isotope
 8 ratios between gas phase and PM is negligible (0.3 ± 0.5 %).

9 Using these assumptions, a set of differential equations was derived that describe the
 10 change in concentration of the isotopologues of the reactant, the intermediate, and the observed
 11 product (Eq. 6 to 9). Here, $^{12}C_{\text{prod/int/pre}}$ and $^{13}C_{\text{prod/int/pre}}$ are the concentrations of each of the ^{12}C
 12 and ^{13}C isotopologues of the product, intermediate and precursor, respectively. $^{12}Y_{\text{int}}$ and $^{13}Y_{\text{int}}$ are
 13 the yields of the intermediate from reaction of the precursor and $^{12}Y_{\text{prod}}$ and
 14 $^{13}Y_{\text{prod}}$ the yields of nitrophenols from reaction of the intermediate phenols. For the sake of
 15 convenience, the reference carbon isotope ratio for the calculations was set to unity and Eq. (9) is
 16 then used to derive δ values from the concentrations of the isotopologues. These carbon isotope
 17 ratios represent the difference between the carbon isotope ratios of precursor emissions and
 18 reaction products. The rate constants k^{12} and k^{13} for different isotopologues can be calculated
 19 from rate constants and the KIE.

20

$$d^{12}C_{\text{prod}} = -^{12}C_{\text{prod}}k_{\text{prod}}^{12}[OH]dt + {}_{\text{prod}}^{12}Y^{12}C_{\text{int}}k_{\text{int}}^{12}[OH]dt \quad \text{Eq. 6a}$$

$$d^{13}C_{\text{prod}} = -^{13}C_{\text{prod}}k_{\text{prod}}^{13}[OH]dt + {}_{\text{prod}}^{13}Y^{13}C_{\text{int}}k_{\text{int}}^{13}[OH]dt \quad \text{Eq. 6b}$$



$$d^{12}C_{int} = -^{12}C_{int}k_{int}^{12}[OH]dt + \frac{^{12}Y^{12}C_{pre}k_{pre}^{12}}{int} [OH]dt \quad \text{Eq. 7a}$$

$$d^{13}C_{int} = -^{13}C_{int}k_{int}^{13}[OH]dt + \frac{^{13}Y^{13}C_{pre}k_{pre}^{13}}{int} [OH]dt \quad \text{Eq. 7b}$$

$$d^{12}C_{pre} = -^{12}C_{pre}k_{pre}^{12}[OH]dt \quad \text{Eq. 8a}$$

$$d^{13}C_{pre} = -^{13}C_{pre}k_{pre}^{13}[OH]dt \quad \text{Eq. 8b}$$

$$\delta^{13}C_{prod} = \left(\frac{^{13}C_{prod}}{^{12}C_{prod}} - 1 \right) \times 1000 \text{ ‰} \quad \text{Eq. 9}$$

1 The largest uncertainty arises from the possible isotope dependence of the yields in Eq. 6
 2 and 7, but uncertainty in kinetic isotope effects also will contribute to uncertainty in the
 3 calculated carbon isotope ratio. Eq. 6 to 9 only describe the fractionation relative to the carbon
 4 isotope ratio of the precursor emissions. In order to determine isotope ratios that can be
 5 compared with observations we use the carbon isotope ratios for emissions reported by Rudolph
 6 et al. (2002). To obtain insight into the possible impact of these uncertainties we use different
 7 scenarios.

8 Since the yields of nitrophenols from the reaction of light aromatic VOC are small, the
 9 feedback of differences in yields for isotopologues of the product on the carbon isotope ratio of
 10 the intermediate is very small and it cannot be distinguished if the isotope fractionation occurs
 11 during formation of the intermediate or the final product. The consequence is that the reaction
 12 channel specific isotope fraction for the formation of nitrophenols is determined by

$$13 \quad \frac{^{13}Y_{xk_{int}}^{13} \times_{int}^{13} Y_{xk_{pre}}^{13}}{^{12}Y_{xk_{int}}^{12} \times_{int}^{12} Y_{xk_{pre}}^{12}} \quad \text{Eq. 10}$$

14 This greatly reduces the number of scenarios that need to be considered.



1 The basic parameters used for solving these differential equations are listed in Table 2.
2 In order to determine the dependence of the calculated isotope ratio on the KIE different
3 scenarios are used. In the first scenario (Scenario 1) it is assumed that formation of nitrophenols
4 is entirely via abstraction of a hydrogen atom from the phenolic OH group and that, since it is a
5 secondary KIE, there is no isotope fractionation from this reaction step. It is also assumed that
6 there is no reaction channel specific isotope fractionation for the formation of the phenolic
7 intermediate from the precursor, This is equivalent to the assumption that ${}_{int}^{12}Y = {}_{int}^{13}Y$ and
8 ${}_{prod}^{12}Yk_{int}^{12} = {}_{prod}^{13}Yk_{int}^{13}$.

9 Another scenario (Scenario 2) is based on the assumption that the isotope fractionation
10 for formation of nitrophenols from the intermediate is identical to the fractionation for all
11 reactions of the intermediate and that there is no reaction channel specific isotope fractionation.
12 It should be noted that for the formation of nitrophenol from the reaction of benzene, the two
13 scenarios will be identical since the reaction of phenol with the OH-radical occurs predominantly
14 via abstraction from the OH group (Atkinson et al., 1992) and it is assumed that this secondary
15 carbon isotope effect is negligible ($k_{int}^{12} = k_{int}^{13}$). For the reactions of toluene and xylene these
16 two scenarios represent an estimate for the upper and lower limit of carbon isotope fractionation
17 resulting from reactions of intermediates.

18 The third scenario (Scenario 3) is based on laboratory studies of the formation of
19 nitrophenols from gas phase reactions of toluene in the presence of NO₂ (Irei et al. 2011; Irei et
20 al., 2015). In these experiments it was found that the $\delta^{13}C$ value of the formed
21 methylnitrophenols is on average 3 ‰ lower than predicted by a mechanistic model assuming
22 that the formation of nitrophenols from cresols is entirely via abstraction of the phenolic
23 hydrogen atom and that this pathway results in no further isotope fractionation between cresols



1 and formed methylnitrophenols. Scenario 3 therefore uses an overall isotope fractionation 3 ‰
2 greater than in Scenario 1. It should be noted that this does not necessarily imply a specific
3 process for the formation of methylnitrophenols from cresols. This 3 ‰ carbon isotope
4 fractionation could be the result of delocalization of the phenolic radical over the aromatic ring
5 structure, which could result in a secondary carbon isotope effect larger than typical secondary
6 isotope effects, an isotope effect for the formation of nitrophenols from the phenoxy radical or a
7 reaction channel specific fractionation during the formation of the phenolic intermediate from the
8 precursor.

9 The results are plotted in Fig. 2 for 2,6-dimethyl-4-nitrophenol, 4-nitrophenol, and 2-
10 methyl-4-nitrophenol together with predictions from mass balance. For comparison the median,
11 10 and 90 percentiles as well as the lowest and highest carbon isotope ratios reported by Saccon
12 at al. (2015) are also shown. For 2-methyl-4-nitrophenol the results of laboratory studies reported
13 by Irei et al. (2015) are included.

14 The predictions by the mechanistic models are very similar for the methylnitrophenol
15 isomers (see example in Fig. S1) and for a wide range of PCAs the difference in predicted carbon
16 isotope ratios between the isomers is less than the estimated accuracy of 0.5 ‰ for carbon
17 isotope ratio measurements of methylnitrophenols (Saccon et al. 2013).

18 For the methylnitrophenols and 2,6-dimethyl-4-nitrophenol in all three scenarios the
19 shape of the dependence between isotope ratio and $\int[\text{OH}]dt$ is very similar and the difference in
20 the intercept with the y-axis is determined by the isotope fractionation specific for the reaction
21 channel resulting in formation of nitrophenols and the kinetic isotope effect for the reaction of
22 the precursor as well as the carbon isotope ratio of precursor emissions.



1 The steep increase in $\delta^{13}\text{C}$ at low values of $\int[\text{OH}]\text{d}t$ is the result of the high reactivity of
2 the phenolic intermediate and the resulting rapid increase in the carbon isotope ratio of the
3 intermediate (Fig. 3). The exception is Scenario 1 for nitrophenol which assumes that the kinetic
4 isotope effect for reaction of phenol with the OH-radical is negligible.

5 At high PCA the dependence between isotope ratio and PCA is nearly linear, representing
6 conditions where the intermediate phenol is in quasi steady state between formation from the
7 precursor and loss reactions (Fig. 3). The PCA ($\int[\text{OH}]\text{d}t$) for transition between the initial steep
8 increase and the nearly linear range depends primarily on the reaction rate constants of the
9 phenolic intermediates. At high values for $\int[\text{OH}]\text{d}t$ the slope of the dependence between $\delta^{13}\text{C}$ and
10 $\int[\text{OH}]\text{d}t$ is mainly determined by the rate constant and kinetic isotope effect for the reaction of
11 the nitrophenol with the OH-radical since most of the aromatic precursor has been consumed
12 (Fig. 3). Nevertheless, due to the continuing formation of nitrophenols from the precursor and
13 the increase in $\delta^{13}\text{C}$ of the precursor this slope is slightly steeper than predicted by the rate
14 constant and kinetic isotope effect for the reaction of the nitrophenol alone. It should be noted
15 that the isotope ratios of the precursor predicted by our mechanistic models are fully consistent
16 with range of carbon isotope ratios of aromatic VOC in the atmosphere reported by Kornilova et
17 al. (2016) (Fig. 3).

18 At high values for $\int[\text{OH}]\text{d}t$ the rate constants or kinetic isotope effects for the loss
19 reaction of nitrophenols have a substantial impact on the dependence between $\delta^{13}\text{C}$ and $\int[\text{OH}]\text{d}t$
20 (see example in Fig.S2). However, as can be seen in Fig. 2 and S2, for the methylnitrophenols
21 and 2,6-dimethyl-4-nitrophenol this range is well outside of the range of the carbon isotope ratios
22 in ambient air reported by Saccon et al. (2015).



1 Rate constants for reaction of the precursor and intermediate with the OH-radical as well
2 as the kinetic isotope effect for reaction of the precursor with the OH-radical have been
3 measured in laboratory studies (see Table 2). Nevertheless, they have some uncertainties that
4 will impact the dependence between carbon isotope ratio and $\int[\text{OH}]dt$. However, for the range of
5 carbon isotope ratios reported by Saccon et al. (2015) the uncertainty of predicted carbon isotope
6 ratios for reasonable errors of measured rate constants and isotope effects is less than 0.5 ‰ (see
7 example in Fig. S3).

8 It is not surprising that the largest uncertainty in the prediction of the dependence
9 between carbon isotope ratio results from the limited knowledge of isotope fractionation effects
10 specific for the reaction channels leading to formation of nitrophenols. For the range of carbon
11 isotope ratios observed in ambient studies uncertainties of the rate constants and kinetic isotope
12 effects known from laboratory studies result in uncertainty of nitrophenol carbon isotope ratios
13 typically less than ± 0.5 ‰, which is similar to or below the estimated accuracy of ambient
14 measurements of nitrophenol carbon isotope ratios (Saccon et al., 2013; Saccon et al., 2015).

15

16 **3.3. Comparison of predicted carbon isotope ratios with laboratory and ambient** 17 **measurements**

18

19 For 2,6 dimethyl-4-nitrophenol and methylnitrophenols, the lower end of mass balance
20 predictions is substantially heavier than the lower end of ambient observations, but for
21 methylnitrophenols mass balance predicts carbon isotope ratios well within the range of the
22 laboratory results reported by Irei et al. (2015). The lower end of carbon isotope ratios predicted
23 by Scenario 1 for 2,6 dimethyl-4-nitrophenol and methylnitrophenols is 3 ‰ to 4 ‰ heavier than



1 the lower end of ambient observations reported by Saccon et al. (2015). Furthermore, six out of
2 the seven carbon isotope ratios of methylnitrophenols observed in laboratory studies by Irei et al.
3 (2015) are more than 2 ‰ lighter than predictions based on Scenario 1.

4 Scenario 3 predicts for 4-nitrophenol at small values of the precursor's PCA ($\int[\text{OH}]dt$
5 $\leq 10^{11}$ s molecules cm^{-3}) that the carbon isotope ratios are lower than the lower limit of ambient
6 observations in an urban area of Toronto (Saccon et al. 2015). Similarly, the methylnitrophenol
7 carbon isotope ratios predicted by Scenario 2 for a $\int[\text{OH}]dt$ of less than 3×10^{10} s molecules cm^{-3}
8 are lighter than the lowest ambient observations (Saccon et al., 2015). Kornilova et al. (2016)
9 reports that 25 % of PCA derived from carbon isotope ratio measurements of benzene and
10 toluene are below 1.1×10^{11} s molecules cm^{-3} and 1.6×10^{10} s molecules cm^{-3} , respectively.
11 However, it has to be considered that for mixing air masses of different PCA, the PCA derived
12 from carbon isotope ratios of the precursor and the reaction product based PCA are not
13 necessarily identical (see 3.5).

14 For high PCA mass balance predicts a substantially lower slope for the dependence
15 between PCA and carbon isotope ratios than all three scenarios based on a mechanistic model.
16 This is due to the conceptual limitation of the mass balance, which does not include the change
17 in carbon isotope ratio resulting from atmospheric reaction of nitrophenols and consequently it
18 cannot be expected that a mass balance can correctly predict carbon isotope ratios at high PCA.

19 There is a substantial range of PCA where $\delta^{13}\text{C}$ can be predicted by a linear
20 approximation. Table 3 shows the regression parameters for Scenarios 2 and 3 for a linear
21 approximation in a range where the difference between exact solution and linear approximation
22 is within the typical measurement accuracy of 0.5 ‰ (Saccon et al., 2013). Except for 4-
23 nitrophenol essentially all of the measurements reported by Saccon et al. (2015) are within the



1 linear range of Scenario 3. Furthermore, for methylnitrophenols and 2,6 dimethyl-4-nitrophenol
2 the slopes of the linear range for different scenarios are, within their uncertainty, identical. This
3 allows determining differences in PCA independent of the scenarios, although the absolute PCA
4 values will be highly dependent on the assumption made for the different scenarios. Based on the
5 estimated accuracy of 0.5 ‰ for nitrophenol carbon isotope ratio measurements, differences in
6 $\int[\text{OH}]dt$ in the range of 6×10^9 s molecules cm^{-3} and 9×10^9 s molecules cm^{-3} can be determined
7 from carbon isotope ratio measurements of alkylnitrophenols. This is similar to the sensitivity of
8 $\int[\text{OH}]dt$ derived from measurement of carbon isotope ratios of toluene (Kornilova et al., 2016).

9

10

11 **3.4. PCA determined from carbon isotope ratios of nitrophenols**

12 Based on the dependence between PCA and carbon isotope ratio of VOC reaction
13 products (Fig. 3) $\int[\text{OH}]dt$ can be determined from measured carbon isotope ratios of ambient
14 nitrophenols under the assumption of a uniform PCA of the observed nitrophenols. The average
15 PCA determined from product isotope ratios are compared in Table 4 with $\int[\text{OH}]dt$ values
16 calculated directly from precursor isotope ratios, which have been published by Kornilova
17 (2012) and Kornilova et al. (2016). The product derived PCA is based on Scenario 3. Scenario 3
18 was chosen since the predicted carbon isotope ratios agree with results from laboratory studies
19 (Fig. 3) and are consistent with the results of available ambient carbon isotope measurements. It
20 should be noted that, although collected at locations only 3 km apart, precursor and product
21 samples were in most cases not collected simultaneously, and in some cases even in different
22 years. Nevertheless, the substantial number of samples in most of the data sets and the low



1 uncertainty of the mean PCA justify a comparison of the precursor derived PCA with $\int[\text{OH}]dt$
2 values calculated from product carbon isotope ratios.

3 Similar to precursor isotope ratio based PCA the product isotope ratio derived PCA
4 increase substantially with decreasing precursor reactivity. This has been explained by Kornilova
5 et al. (2016) by mixing of air masses with different PCA, which results in a lower weight for
6 VOC with high reactivity in aged air due to faster photochemical removal. However, the
7 weighting of contributions from different air masses differs between precursor isotope ratio
8 derived PCA and product isotope ratio derived PCA. Details will be discussed in Section 3.5.

9 All precursor isotope ratio derived PCA differ significantly from the PCA determined
10 from nitrophenol carbon isotope ratios. Toluene and xylene precursor derived PCA are lower
11 than reactant derived PCA by approximately 4×10^{10} s molecules cm^{-3} and 3×10^{10} s molecules
12 cm^{-3} , respectively. The average PCA derived from 4-nitrophenol carbon isotope ratios is
13 approximately 50 % higher than the average PCA calculated from benzene carbon isotope ratios.

14 Uncertainty of the calculated average PCA can result from uncertainty of parameters used
15 to calculate PCA from carbon isotope ratios. The 10 percentiles and the 90 percentiles of
16 nitrophenol isotope ratios range from approximately -36 % to -31 %. For this range errors of
17 rate constants and kinetic isotope effects for reactions of the precursors or the nitrophenols only
18 have a small impact on the dependence between PCA and carbon isotope ratio (Fig. S2 and S3)
19 and therefore cannot explain the difference in average PCA. Changes in the carbon isotope ratios
20 of VOC emissions as well as the isotope fractionation for reactions or branching of the
21 intermediates in the reaction sequence resulting in nitrophenol formation can have a significant
22 impact on PCA calculated from nitrophenol carbon isotope ratios (Table 5).



1 However, PCA derived from precursor's carbon isotope ratio measurements also strongly
2 depend on the carbon isotope ratios of the emissions (Kornilova et al., 2016). For a decrease in
3 emission isotope ratios of 1 ‰ the PCA derived from carbon isotope ratios of benzene, toluene
4 and m-xylene increase by 0.9×10^{11} s molecules cm^{-3} , 0.3×10^{11} s molecules cm^{-3} , and 0.09×10^{11} s
5 molecules cm^{-3} , respectively. Consequently, a decrease in the carbon isotope ratio of emission by
6 1 ‰ would reduce the difference between precursor and product derived PCA for benzene,
7 toluene and xylene by approximately 0.7×10^{11} s molecules cm^{-3} , 0.15×10^{11} s molecules cm^{-3} , and
8 less than 0.01×10^{11} s molecules cm^{-3} , respectively. An approximately 3 ‰ decrease in the
9 carbon isotope ratio of toluene emissions would be able to explain the difference in PCA derived
10 from toluene carbon isotope ratios and methylnitrophenol carbon isotope ratios. Similarly, an
11 increase in the carbon isotope ratio of benzene emissions by 2.5 ‰ would eliminate the
12 difference between benzene and 4-nitrophenol derived PCA. However, a 2-3 ‰ error in the
13 carbon isotope ratio of emissions is substantially larger than the uncertainty derived from VOC
14 emission studies (Rudolph et al., 2002; Rudolph, 2007; Kornilova et al., 2016). Moreover, a
15 carbon isotope ratio of benzene emissions heavier by 2.5 ‰ than the value used in our
16 calculations (Table 2) would not be compatible with the lower end of ambient benzene carbon
17 isotope ratios reported by Kornilova et al. (2016). The discrepancies between the m,p-xylene and
18 2,6-dimethyl-4-nitrophenol derived PCA cannot be explained by uncertainty of the carbon
19 isotope ratios of xylene emissions. However, it should be noted that the precursor based PCA is
20 derived from ambient observations of the combined isotope ratios of p-xylene and m-xylene,
21 whereas only m-xylene is precursor of 2,6-dimethyl-4-nitrophenol.

22 An increase in the carbon isotope fractionation specific for the formation of nitrophenols
23 from the intermediate phenol of approximately 3 ‰ would result in very good agreement



1 between precursor and product derived PCA for toluene and xylene. However, for the conditions
2 of the laboratory studies reported by Irei et al. (2015) a model with such an additional isotope
3 fractionation for the formation of nitrophenols from reaction of the intermediate would predict
4 methylnitrophenol isotope ratios for the 7 laboratory measurements reported by Irei et al. (2015),
5 which are on average by 2.5 ‰ lighter than the measured values. Based on the reported average
6 experimental uncertainty of less than 1 ‰ this difference is significant at a higher than 99.9 %
7 confidence level.

8 For the formation of 2,6-dimethyl-4-nitrophenol from m-xylene no laboratory results are
9 available, which would allow constraining carbon isotope fractionation for reactions of the
10 intermediate phenol. However, it is unlikely that carbon isotope fractionation for reactions of the
11 intermediate dimethyl phenol are substantially larger than for the cresol intermediates.

12 The formation of 4-nitrophenol from atmospheric oxidation of benzene proceeds via
13 phenol, which reacts with OH-radicals, in contrast to methyl substituted phenols, primarily by H-
14 abstraction from the phenol group. Consequently, a reaction channel specific carbon isotope
15 fractionation substantially different from that for reactions of methyl substituted phenols cannot
16 be ruled out. However, a model scenario that would result in good agreement between precursor
17 and product derived average PCA for benzene would also predict that the lowest carbon isotope
18 ratio for 4-nitrophenol is significantly higher than approximately 30 % of the measured ambient
19 carbon isotope ratios reported by Saccon et al. (2015).

20 In addition to the formation of nitrophenols via OH-radical initiated oxidation, reaction
21 of the intermediate cresol with NO₃ also has to be considered a possible reaction pathway for the
22 formation of the methylnitrophenols (Carter et al., 1981). Here, it was proposed that at NO_x



1 levels greater than 20 ppb and ozone levels much larger than NO levels, the reaction with NO₃
2 would dominate over the proposed reaction with OH-radicals. However, since [OH] and [NO₃]
3 each exhibit very pronounced diurnal cycles, with [OH] peaking during the day and [NO₃]
4 peaking at night due to its fast photolysis during daytime, reactions with NO₃ during the day can
5 be ignored. The proposed reaction pathway of the cresol + NO₃ reaction is through an addition
6 reaction, resulting in a similar estimated KIE as the addition of the OH group. Consequently, the
7 carbon isotope ratio of nitrophenols formed via this reaction pathway will not depend
8 significantly on the formation pathway. However, due to the possible nighttime processing of the
9 phenolic intermediate in the presence of NO₃ this may create a difference between the true value
10 for $\int[\text{OH}]dt$ and the PCA derived from the carbon isotope ratio of the nitrophenol. To determine
11 this possible bias Scenario 3 was modified. At a value for $\int[\text{OH}]dt$ corresponding to the average
12 carbon isotope ratios reported by Saccon et al. (2015) the OH radical concentration was set to
13 zero and replaced by a mechanism representing reaction of the intermediate at 1 pmol mol⁻¹ of
14 NO₃ until the phenolic intermediate was nearly completely depleted. The resulting average bias
15 in $\int[\text{OH}]dt$ is less than 0.2 % for all of the methylnitrophenol isomers when compared to the
16 unmodified Scenario 3.

17 The reactions of cresols with OH-radicals is substantially faster than the formation of
18 cresols from reaction of toluene with OH-radicals. This does not allow the build-up of high
19 concentrations of cresols during the day. This limits the possible role of the NO₃ reaction
20 pathway. For the same reason it is unlikely that the NO₃ reaction pathway plays a substantial role
21 for the formation of 4-nitrophenol or 2,6-dimethyl-4-nitrophenol.

22 The sensitivity estimates above are based on the range of nitrophenol carbon isotope
23 ratios reported by Saccon et al. (2015). For isotope ratios outside of this range, errors in PCA



1 caused by uncertainty of the parameters used for calculating $\int[\text{OH}]dt$ may differ. While there is
2 an effectively linear dependence between PCA and carbon isotope ratio for a range of
3 approximately 5 to 8 ‰ for the mechanistic models (Fig. 3, Table 2), eventually the slope of the
4 dependence of carbon isotope ratio on PCA begins to decrease substantially (Fig. 3). In this
5 region, a change in carbon isotope ratio or one of the model parameters could result in a larger
6 change in PCA than for low carbon isotope ratios. However, the region of decreasing sensitivity
7 depends strongly on precursor reactivity. For Scenario 3 this occurs at approximately 5×10^{10} s
8 molecules cm^{-3} in the case of 2,6-dimethyl-4-nitrophenol and 3×10^{11} s molecules cm^{-3} in the case
9 of 4-nitrophenol.

10 Figure 7 shows the frequency distributions for PCA determined from the carbon isotope
11 ratios of 4-nitrophenol (Fig. 4a) and methylnitrophenols (Fig. 4b) using Scenario 3. For
12 comparison percentiles for PCA derived from carbon isotope ratios of benzene (Fig. 4a) and
13 toluene (Fig. 4b) reported by Kornilova et al. (2016) are also shown. Consistent with the
14 difference in average PCA (Table 4), PCA derived from 4-nitrophenol carbon isotope ratios are
15 shifted approximately 2×10^{11} s molecules cm^{-3} towards higher values than PCA derived from
16 benzene carbon isotope ratios, but the width of the two PCA distributions are very similar
17 (Fig.4a). In contrast to this the PCA distribution derived for methylnitrophenols is, compared to
18 the toluene derived distribution, not only shifted to lower values, but also much narrower (Fig.
19 4b). While uncertainty of the assumptions made to determine the dependence between PCA and
20 carbon isotope ratios of nitrophenols can to some extent explain the difference in average PCA it
21 cannot explain a substantial difference in the width of the distributions since nearly all observed
22 carbon isotope ratios are within or close to the linear range of dependencies between nitrophenol
23 carbon isotope ratio and PCA (Fig. 2, Table 3).



1 3.5. Average PCA and mixing of air masses

2

3 Based on measurement of carbon isotope ratios of several aromatic VOC (Canada)
4 Kornilova et al. (2016) concluded that mixing ratios and average PCA of aromatic VOC in
5 Toronto typically are determined by mixing of air masses with VOC of different origin and
6 different PCA. While $\int[\text{OH}]dt$ determined from the isotope ratios of aromatic VOC represent for
7 all practical purposes the correct concentration weighted average PCA for the studied VOC
8 (Rudolph and Czuba, 2000; Kornilova et al., 2016), the situation is different for PCA derived
9 from isotope ratios of VOC reaction products such as nitrophenols. In case of atmospheric
10 mixing of VOC and VOC reaction products the PCA derived from product carbon isotope ratios
11 can differ from $\int[\text{OH}]dt$ calculated for VOC isotope ratios for several reasons.

12 For nitrophenols with different PCA the decrease in sensitivity of the PCA-carbon
13 isotope ratio dependence outside of the linear range (Fig. 3, Table 3) will reduce the apparent
14 PCA derived from nitrophenols compared to the VOC derived PCA. On the other hand, with
15 increasing PCA the VOC precursor concentrations will not only decrease due to atmospheric
16 dilution, but also due to chemical reactions, which reduces their weight for average PCA. In
17 contrast to this nitrophenols are formed as result of precursor reactions, which will counteract the
18 effect of atmospheric dilution. However, in contrast to light aromatic hydrocarbons the polar
19 nitrophenols are water soluble and can be found both in the particle and gas phase (Saccon et al.,
20 2013). Consequently, they will be removed not only by chemical reactions, but also by wet and
21 dry deposition. Carbon isotope fractionation resulting from physical removal processes is much
22 smaller than isotope fractionation during chemical reactions and therefore will have little direct
23 impact on the carbon isotope ratio of nitrophenols but physical removal processes will reduce the



1 concentration of nitrophenols in aged air masses and therefore reduce the weight of aged air in
2 samples representing air masses with different PCA. Combined, these effects can create a
3 complex situation with sometimes substantial differences in PCA derived from precursor isotope
4 ratios compared to nitrophenol derived PCA.

5 Nevertheless, a simple general consequence of the mixing of aged air with fresh
6 emissions of light aromatic VOC is the absence of very low values for 4-nitrophenol derived
7 PCA whereas in the case of dominant fresh emissions values close to zero can be expected for
8 precursor derived PCA (Fig. S4a). This is the consequence of the delay in formation of
9 nitrophenols following precursor emissions although details on how PCA are impacted by the
10 influence of aged air masses depends on details of mixing as well as the possible removal of
11 nitrophenols by deposition (Fig. S4b). The 4-nitrophenol depositional loss rates used for the
12 calculations are relative to the removal of 4-nitrophenol by reaction with the OH-radical,
13 although it must be considered that loss by deposition will be independent of the OH-radical
14 concentration. However, the actual impact of deposition on the PCA will only depend on the
15 relative contribution of deposition to the overall 4-nitrophenol loss since this will influence the
16 weight an air mass with a given PCA will have on the average PCA. For an average OH-radical
17 concentration of 10^6 molecules cm^{-3} a deposition loss equal to the photochemical 4-nitrophenol
18 loss rate corresponds to a deposition lifetime of approximately 6 weeks and a total lifetime of 3
19 weeks. For depositional loss 10 times faster than chemical removal the 4-nitrophenol lifetime is
20 approximately 4 days.

21 While conceptually mixing of two air masses with different PCA explains the difference
22 in the frequency of observations of very low PCA between precursor and product derived PCA,
23 it can be expected that for urban sites a range of PCA will be a more realistic situation. For the



1 average precursor derived PCA the distribution for individual PCA observations is known
2 (Kornilova et al., 2016). For comparison of the average PCA we use these distributions to
3 calculate the PCA distribution for 4-nitrophenol and understand the source of differences in the
4 average PCA.

5 Figure 5 shows the resulting PCA distributions calculated for different depositional loss
6 rates of 4-nitrophenol. With increasing loss by deposition, the centers of the distributions shift
7 towards lower PCA and become narrower, which is the consequence of decreasing contributions
8 of air-masses with high PCA. The center of the distribution resulting from a depositional loss
9 rate five times faster than loss due to reaction with the OH-radical has its maximum at a value for
10 $[\text{OH}]/\text{dt}$ of approximately $5 \times 10^{11} \text{ s molecules cm}^{-3}$, which is close to the average of PCA derived
11 from observed 4-nitrophenol isotope ratios (Table 4).

12 A comparison of calculated distributions with the carbon isotope ratio derived PCA
13 distributions shows that not only the averages but also the widths of the distributions agree for
14 depositional loss rates of 4-nitrophenol between three and seven times faster than reaction with
15 the OH-radical (Fig. 6) within the statistical errors of the observations. Based on an average OH-
16 radical concentration of $10^6 \text{ radicals cm}^{-3}$ the 4-nitrophenol loss by deposition corresponds to a
17 life time in the range of 6 days to 2 weeks. To our knowledge there are no published values for
18 wet or dry deposition rates of 4-nitrophenol, but the relatively low deposition rates are consistent
19 with the observation that only a small fraction of atmospheric 4-nitrophenol is found in the
20 particle phase (Saccon et al., 2013).

21 The contribution of an air mass with a given PCA derived from 4-nitrophenol carbon
22 isotope ratios depends on the deposition rate relative to the rate of reaction of 4-nitrophenol and



1 the benzene precursor with the OH-radical. However, there is no direct connection between
2 deposition rates and the reaction rate with OH-radicals and therefore for individual observations
3 the ratio of depositional loss rate over the impact of OH-radical chemistry can vary substantially.
4 For example, during rain events it can be expected that deposition will be faster than on average
5 whereas removal as well as formation of 4-nitrophenol due to reaction with OH-radicals will be
6 slower.

7 Indeed, rain has a substantial impact on the atmospheric concentrations of nitrophenols in
8 the particle phase as well as in the gas phase. Substantial precipitation during sampling or on the
9 day before sampling, reduces the nitrophenol concentrations by a factor between 3 and 6 (Fig.
10 7a). In contrast, precipitation has no significant impact on PCA (Fig. 7b). Changes in PCA are
11 within the uncertainty of the averages for different precipitation conditions and, except for 4-
12 methyl-2-nitrophenol below 25%. This is consistent with the assumption that deposition is an
13 important loss process for atmospheric nitrophenols, and that deposition does not result in
14 significant carbon isotope fractionation of nitrophenols.

15 For the precursor of methylnitrophenols, toluene, the PCA distribution is very different
16 from the distribution observed for benzene, the precursor of 4-nitrophenol (Kornilova et al.,
17 2016). The average PCA for toluene is approximately only one third of the benzene PCA and the
18 distribution peaks PCA close to zero, indicating a strong influence from very recent toluene
19 emissions. The different behavior of benzene and toluene has been explained by the difference in
20 reactivity and the different geographical distribution of emission sources (Kornilova et al., 2016).
21 There are substantial sources of toluene within the area of Metropolitan Toronto, whereas most
22 major sources of benzene are located in the surrounding regions.



1 The low average PCA derived from methylnitrophenol isotope ratios is consistent with a
2 dominant role of local emissions of toluene and demonstrates that air masses containing
3 methylnitrophenols with high PCA are only of limited importance in determining the
4 methylnitrophenol PCA. This is supported by the dependence of methylnitrophenol
5 concentrations, carbon isotope ratios and PCA on wind speed shown in Fig. 8 and 9.

6 Figure 8 indicates that when the maximum wind speed over the sampling time is lowest,
7 concentrations for 2-methyl-4-nitrophenol are highest and the corresponding isotope ratios are
8 lowest, indicating that methylnitrophenols may be dominantly produced from local emissions
9 with limited mixing. This is consistent with the observed PCA (Fig. 9), which is lowest when
10 wind speed is lowest and increases with increasing wind speed. This can be explained by a
11 decrease of the impact of local emissions resulting in a larger relative contribution of aged 2-
12 methyl-4-nitrophenol originating from further away. A similar trend is observed for 3-methyl-4-
13 nitrophenol. 4-methyl-2-nitrophenol and 2,6-dimethyl-4-nitrophenol were not considered due to
14 the small number of samples. 4-nitrophenol did not show any systematic trend. This is
15 consistent, with the, compared to toluene, lower reactivity of benzene, the 4-nitrophenol
16 precursor and the lower local emission rates for benzene (Kornilova et al., 2016). Both factors
17 will greatly diminish the role of local emission and local photochemistry on the average PCA
18 derived from 4-nitrophenol carbon isotope ratios.

19 **4 Summary and Conclusions**

20 Similar to primary emissions of VOC for secondary pollutants PCAs derived from carbon
21 isotope ratios decreases with increasing reactivity. This allows probing atmospheric processing
22 of pollutants at different timescales and consequently differentiating between impact from local



1 emission and long-range transport. In principle carbon isotope ratios of secondary organic
2 pollutants provide better insight into the formation of secondary products than carbon isotope
3 ratios of precursors. However, currently the use of carbon isotope ratios of secondary organic
4 pollutants is limited by uncertainties and gaps in understanding of the formation mechanism and
5 the carbon isotope fractionation during the reaction sequence.

6 Using available published ambient observations of precursor and reactant isotope ratios
7 as well as results of a published laboratory study of isotope ratios of the photochemical oxidation
8 products of toluene it was possible to identify the most plausible scenario for a mechanistic
9 model describing the dependence between carbon isotope ratios of atmospheric nitrophenols, and
10 atmospheric processing of their precursors, light aromatic VOC.

11 Mixing of air masses with nitrophenols of different values for $\int[\text{OH}]dt$ plays an important
12 role in determining their carbon isotope ratios and needs to be considered in the interpretation of
13 carbon isotope ratios of secondary organic pollutants and the relation between concentrations and
14 carbon isotope ratios. Although deposition will not have a substantial direct impact on the carbon
15 isotope ratios of nitrophenols, deposition of nitrophenols plays a major role in determining the
16 atmospheric residence time of nitrophenols in the atmosphere. Consequently, the dependence
17 between atmospheric residence time and carbon isotope ratios of nitrophenols results in a strong
18 dependence between average nitrophenol PCA and deposition rate. The dependence of
19 deposition rate on factors only weakly related to photochemical reactivity of the atmosphere can
20 explain the absence of a significant dependence between the concentration of nitrophenols and
21 their carbon isotope ratios. Similarly, dispersion in the atmosphere has an indirect, but visible
22 impact not only on the concentration of nitrophenols, but also on their carbon isotope ratios. It
23 should be noted that these results are based on observations in a major urban area with



1 substantial local and regional nitrophenol precursor emissions and are not necessarily correct for
2 regions without substantial emission sources for the light aromatic compounds.

3

4 **Acknowledgements**

5 The authors would like to thank Darrell Ernst and Wendy Zhang from Environment & Climate
6 Change Canada for their technical support. This research was supported financially by the
7 Natural Sciences and Engineering Research Council of Canada (NSERC) and the Canadian
8 Foundation for Climate and Atmospheric Sciences (CFCAS).

9 **References**

- 10 Anderson, R.S., Iannone, R., Thompson, A. E., Rudolph, J., Huang, L.: Carbon kinetic isotope
11 effects in the gas-phase reactions of aromatic hydrocarbons with the OH radical at 296 ± 4 K,
12 *Geophys. Res. Lett.*, 31, L15108, doi:10.1029/2004GL020089, 2004.
- 13 Atkinson, R.: Atmospheric chemistry of VOCs and NO_x, *Atmos. Environ.* 34, 2063-2101, 2000.
- 14 Atkinson, R. and Aschmann, S.M.: Rate constants for the gas-phase reactions of the OH radical
15 with the cresols and dimethylphenols at 296 ± 2 K, *Int. J. Chem. Kinet.*, 22, 59-67, 1990.
- 16 Atkinson, R., Carter, W.P.L., Darnall, K.R., Winer, A.M., Pitts, J.N. Jr.: A smog chamber and
17 modeling study of the gas phase NO_x-air photooxidation of toluene and the cresols, *Int. J.*
18 *Chem. Kinet.*, 12, 779-836, 1980.
- 19 Atkinson, R., Aschmann, S.M. and Arey, J.: Reactions of OH and NO₃ radicals with phenol,
20 cresols, and 2-nitrophenol at 296 ± 2 K, *Environ. Sci. & Technol.*, 26, 1397-1403, 1992.
- 21 Bejan, I., Barnes, I., Olariu, R., Zhou, S., Wiesen, P., Benter, T.: Investigations on the gas-phase
22 photolysis and OH radical kinetics of methyl-2-nitrophenols, *Phys. Chem. Chem. Phys.*, 9,
23 5686-5692, 2007.
- 24 Calvert, J.G., Atkinson, R., Becker, K.H., Kamens, R.M., Seinfeld, J.H., Wallington, T.J.,
25 Yarwood, G.: The mechanisms of atmospheric oxidation of aromatic hydrocarbons, Oxford
26 University Press, New York, USA, 2002.
- 27 Carter, W.P.L., Winer, A.M., Pitts, J.N. Jr.: Major atmospheric sink of phenol and the cresols.
28 Reaction with the nitrate radical, *Environ. Sci. Technol.*, 15, 829-831, 1981.
- 29 Czapiewski, K., Czuba, E., Huang, L., Ernst, D., Norman, A.L., Koppmann, R., Rudolph, J.:
30 Isotopic composition of non-methane hydrocarbons in emissions from biomass burning, J.
31 *Atmos. Chem.*, 43, 45-60, 2002.



- 1 Forstner, H., Flagan, R. and Seinfeld, J.: Secondary organic aerosol from the photooxidation of
2 aromatic hydrocarbons: Molecular composition, *Environ. Sci. & Technol.*, 31, 1345-1358,
3 1997.
- 4 Gensch, I., Kiendler-Scharr, A. and Rudolph, J.: Isotope ratio studies of atmospheric organic
5 compounds: principles, methods, applications and potential, *Int. J. Mass Spectrom.*, 365-366,
6 206-221, 2014.
- 7 Goldstein, A. and Shaw, S.: Isotopes of volatile organic compounds: An emerging approach for
8 studying atmospheric budgets and chemistry, *Chem. Rev.*, 103, 5025-5048, 2003.
- 9 Grosjean, D.: Atmospheric fate of toxic aromatic compounds, *Sci. Total Environ.*, 100, 367-414,
10 1991.
- 11 Gundel, L. and Herring, S.V.: Absorbing filter media for denuder-filter sampling of total organic
12 carbon in airborne particles, Record of invention WIB 1457, Lawrence Berkeley National
13 Laboratory, USA, 1998.
- 14 Hamilton, J., Webb, P., Lewis, A., Reviejo, M.: Quantifying small molecules in secondary
15 organic aerosol formed during the photo-oxidation of toluene with hydroxyl radicals, *Atmos.*
16 *Environ.*, 39, 7263-7275, 2005.
- 17 Harrison, M.A.J., Heal, M.R. and Cape, J.N.: Evaluation of the pathways of tropospheric
18 nitrophenol formation from benzene and phenol using a multiphase model, *Atmos. Chem.*
19 *Phys.*, 5, 1679-1695, doi:10.5194/acp-5-1679-2005, 2005.
- 20 Herrmann, H., Exner, M., Jacobi, H-W., Raabe, G., Reese, A., Zellner, R.: Laboratory studies of
21 atmospheric aqueous-phase free-radical chemistry: Kinetic and spectroscopic studies of
22 reactions of NO₃ and SO₄⁻ radicals with aromatic compounds, *Faraday Discuss.*, 100, 129-
23 153, 1995.
- 24 Inomata, S., Tanimoto, H., Fujitani, Y., Sekimoto, K., Sato, K., Fushimi, A., Yamada, H., Hori,
25 S., Kumazawa, Y., Shimono, A., Hikida, T.: On-line measurements of gaseous nitro-organic
26 compounds in diesel vehicle exhaust by proton-transfer-reaction mass spectrometry, *Atmos.*
27 *Environ.*, 73, 195-203, 2013.
- 28 Inomata, S., Fushimi, A., Sato, K., Fujitani, Y., Yamada, H.: 4-nitrophenol, 1-nitropyrene, and 9-
29 nitroanthracene emissions in exhaust particles from diesel vehicles with different exhaust gas
30 treatments, *Atmos. Environ.*, 110, 93-102, 2015.
- 31 Irei, S., Huang, L., Collin, F., Zhang, W., Hastie, D., Rudolph, J.: Flow reactor studies of the
32 stable carbon isotope composition of secondary particulate organic matter generated by OH-
33 radical-induced reactions of toluene, *Atmos. Environ.* 40, 5858–5867, 2006.
- 34 Irei, S., Rudolph, J., Huang, L., Auld, J., Hastie, D.: Stable carbon isotope ratio of secondary
35 particulate organic matter formed by photooxidation of toluene in indoor smog chamber,
36 *Atmos. Environ.*, 45, 856-862, 2011.
- 37 Irei, S., Rudolph, J., Huang, L.: Compound-specific stable carbon isotope ratios of phenols and
38 nitrophenols derivatized with N,O-bis(trimethylsilyl)trifluoroacetamide, *Anal. Chim. Acta*,
39 786, 95-102, 2013.
- 40 Irei, S., Rudolph, J., Huang, L., Auld, J., Collin, F., Hastie, D.: Laboratory Studies of Carbon
41 Kinetic Isotope Effects on the Production Mechanism of Particulate Phenolic Compounds



- 1 Formed by Toluene Photooxidation: A Tool to Constrain Reaction Pathways, *J. Phys. Chem.*,
2 119, 5-13, 2015.
- 3 Jang, M. and Kamens, R.: Characterization of secondary aerosol from the photooxidation of
4 toluene in the presence of NO_x and 1-Propene, *Environ. Sci. Technol.*, 35, 3626-3639, 2001.
- 5 Jobson, B.T., Parrish, D.D., Goldan, P., Kuster, W., Fehsenfeld, F.C., Blake, D.R., Blake, N.J.,
6 Niki, H.: Spatial and temporal variability of nonmethane hydrocarbon mixing ratios and their
7 relation to photochemical lifetime, *J. Geophys. Res.*, 103, 13557-13567, 1998.
- 8 Jobson, B.T., McKeen, S.A., Parrish, D.D., Fehsenfeld, F.C., Blake, D.R., Goldstein, A.H.,
9 Schaufli, S.M., Elkins, J.W.: Trace gas mixing ratio variability versus lifetime in the
10 troposphere and stratosphere: Observations, *J. Geophys. Res.*, 104, 16091-16113, 1999.
- 11 Kleinman, L.I., Daum, P.H., Lee, Y.N., Nunnermacker, L.J., Springston, S.R., Weinstein-Lloyd,
12 J., Hyde, P., Doskey, P., Rudolph, J., Fast, J., Berkowit, C.: Photochemical age determinations
13 in the Phoenix metropolitan area, *J. Geophys. Res.*, 108, 4096, 2003.
- 14 Kornilova, A., Saccon, M., O'Brien, J.M., Huang, L., Rudolph, J.: Stable carbon isotope ratios
15 and the photochemical age of atmospheric volatile organic compounds, *Atmos. Ocean*, 53, 7-
16 13, 2013.
- 17 Kornilova, A.: Stable carbon isotope composition of ambient VOC and its use in the
18 determination of photochemical ages of air masses, Ph.D. thesis, York University, Toronto,
19 ON, 2012.
- 20 Kornilova, A., Saccon, M., Huang, L., Rudolph, J.: Stable carbon isotope ratios of ambient
21 aromatic volatile organic compounds, *Atmos. Chem. Phys.*, 16, 111755-11772, 2016
- 22 Moukhtar, S., Saccon, M., Kornilova, A., Irei, S., Huang, L., Rudolph, J.: Method for
23 determination of stable carbon isotope ratio of methylnitrophenols in atmospheric particulate
24 matter, *Atmos. Meas. Tech.*, 4, 2453-2464, 2011.
- 25 Parrish, D.D., Hahn, C.J., Williams, E.J., Norton, R.B., Fehsenfeld, F.C., Singh, H.B., Shetter,
26 J.D., Gandrud, B.W., Ridley, B.A.: Indications of photochemical histories of Pacific air
27 masses from measurements of atmospheric trace species at Point Area, California, *J.*
28 *Geophys. Res.*, 97, 15,883-15,901, 1992.
- 29 Parrish, D.D., Stohl, A., Forster, C., Atlas, E.L., Blake, D.R., Goldan, P.D., Kuster, W.C., de
30 Gouw, J.A.: Effects of mixing on evolution of hydrocarbon ratios in the troposphere, *J.*
31 *Geophys. Res.*, 112, D10S34, doi:10.1029/2006JD007583, 2007.
- 32 Rudolph, J.: Gas Chromatography-Isotope Ratio Mass Spectrometry, in: Volatile organic
33 compounds in the atmosphere, edited by: Koppmann, R., Blackwell Publishing Ltd, UK, 388-
34 466, 2007.
- 35 Rudolph, J. and Czuba, E.: On the use of isotopic composition measurements of volatile organic
36 compounds to determine the "photochemical age" of an air mass, *Geophys. Res. Letts.*, 27,
37 3865-3868, 2000.
- 38 Rudolph, J., Czuba, E., and Huang, L.: The stable carbon isotope fractionation for reactions of
39 selected hydrocarbons with OH-radicals and its relevance for atmospheric observations in an
40 urban atmosphere, *J. Geophys. Res.*, 10, 29329-29346, 2000.
- 41 Rudolph, J., Czuba, E., Norman, A.L., Huang, L., Ernst, D.: Stable carbon isotope composition
42 of nonmethane hydrocarbons in emissions from transportation related sources and
43 atmospheric observations in an urban atmosphere, *Atmos. Environ.*, 36, 1173-1181, 2002.
- 44 Rudolph, J., Anderson, R.S., Czapiewski, K.V., Czuba, E., Ernst, D., Gillespie, T., Huang, L.,
45 Rigby, C., Thompson, A.E.: The stable carbon isotope ratio of biogenic emissions of isoprene



- 1 and the potential use of stable isotope ratio measurements to study photochemical processing
2 of isoprene in the atmosphere, *J. Atmos. Chem.*, 44, 39-55, 2003.
- 3 Saccon, M., Busca, R., Facca, C., Huang, L., Irei, S., Kornilova, A., Lane, D., Rudolph, J.:
4 Method for the determination of concentration and stable carbon isotope ratios of atmospheric
5 phenols, *Atmos. Meas. Tech.*, 6, 2969-2974, 2013.
- 6 Saccon, M., Kornilova, A., Huang, L., Moukhtar, S., Rudolph, J.: Stable carbon isotope ratios of
7 ambient secondary organic aerosols in Toronto, *Atmos. Chem. Phys.*, 15, 10825-10838, 2015.
- 8 Sato, K., Hatakeyama, S., Imamura, T.: Secondary organic aerosol formation during the
9 photooxidation of toluene: NO_x dependence of chemical composition, *J. Phys. Chem. A*, 111,
10 9796-9808, 2007.
- 11 Spivakovsky, C.M., Logan, J.A., Montzka, S.A., Balkanski, Y.J., Foreman-Fowler, M., Jones,
12 D.B.A., Horowitz, L.W., Fusco, A.C., Brenninkmeijer, C.A.M., Prather, M.J., Wofsy, S.C.,
13 McElroy, M.B.: Three-dimensional climatological distribution of tropospheric OH: Update
14 and evaluation, *J. Geophys. Res.*, 105, 8931-8980, 2000.
- 15 Stein, O. and Rudolph, J.: Modeling and interpretation of stable carbon isotope ratios of ethane
16 in global chemical transport models, *J. Geophys. Res.*, 112, D14308,
17 doi:10.1029/2006JD008062, 2007.
- 18 Thompson, A.: Stable carbon isotope ratios of nonmethane hydrocarbons and halocarbons in the
19 atmosphere, Ph.D. thesis, York University, Toronto, ON, 2003.
- 20 Tremp, J., Mattrel, P., Fingler, S., Giger, W.: Phenols and nitrophenols as tropospheric
21 pollutants: emissions from automobile exhausts and phase transfer in the atmosphere, *Water*
22 *Air Soil Poll.*, 68, 113-123, 1993.
- 23
- 24



1 Tables

2 **Table 1.** Parameters, including the rate constant of the precursor with the OH radical (k_{OH}), KIE
 3 and the isotope ratio of emissions ($\delta^{13}\text{C}_0$) used for the determination of the PCA by Eq. (5). The
 4 uncertainty of the parameter is given in parenthesis.

	Precursor		Product	Product Abbreviation
Benzene	k_{OH}^{a} ($\text{cm}^3 \text{ molec}^{-1} \text{ s}^{-1}$)	1.39×10^{-12}	4-nitrophenol	4-NP
	ϵ^{b} (‰)	7.83 (0.42)		
	$\delta^{13}\text{C}_0^{\text{c}}$ (‰)	-28.0 (0.2)		
Toluene	k_{OH}^{a} ($\text{cm}^3 \text{ molec}^{-1} \text{ s}^{-1}$)	5.63×10^{-12}	4-methyl-2-nitrophenol	4-me-2-NP
	ϵ^{b} (‰)	5.95 (0.28)	3-methyl-4-nitrophenol	3-me-4-NP
	$\delta^{13}\text{C}_0^{\text{c}}$ (‰)	-27.6 (0.5)	2-methyl-4-nitrophenol	2-me-4-NP
m-Xylene	k_{OH}^{a} ($\text{cm}^3 \text{ molec}^{-1} \text{ s}^{-1}$)	2.31×10^{-11}	2,6-dimethyl-4-nitrophenol	2,6-dime-4-NP
	ϵ^{b} (‰)	4.83 (0.05)		
	$\delta^{13}\text{C}_0^{\text{c}}$ (‰)	-27.4 (0.4)		

5 ^a Calvert et al., 2002, uncertainty not included since the uncertainty resulting from error in the rate
 6 constants is small compared to uncertainties derived from error in the isotope ratio and KIE. ^b Anderson et
 7 al. (2004). ^c Rudolph et al. (2002); for m-xylene the value reported for p+m-xylene is given.

8



Table 2. Parameters used to determine the PCA for individual products. Units of k (rate constant) are in $\text{cm}^3 \text{ molecule}^{-1} \text{ s}^{-1}$. Since 80 % of the phenols are in the gas phase (Saccon et al., 2013), the rate constant for the product loss was adjusted to 80 % of the gas phase rate constant. If available, the uncertainty of the parameter is given in parenthesis.

	Precursor		Intermediate		Product (Gas + PM)	
	k^a	ϵ_{OH}^b (%) $\delta^{13}\text{C}_0^c$ (%)	k^a	ϵ_{OH}^d (%)	k^e	ϵ_{OH}^f (%)
Benzene	1.39×10^{-12}	7.83 (0.42) -28.0 (0.2)	Phenol	0	4-NP	3.40×10^{-13} 5.36
Toluene	5.63×10^{-12}	5.95 (0.28) -27.6 (0.5)	4-me-phenol	5.47	4-me-2-NP	2.87×10^{-12} 5.95
Toluene	5.63×10^{-12}	5.95 (0.28) -27.6 (0.5)	3-me-phenol	5.47	3-me-4-NP	2.92×10^{-12} 5.95
Toluene	5.63×10^{-12}	5.95 (0.28) -27.6 (0.5)	2-me-phenol	5.47	2-me-4-NP	2.87×10^{-12} 5.95
m-xylene	2.31×10^{-11}	4.83 (0.05) -27.4 (0.4)	2,6-dime-phenol	4.83	2,6-dime-4-NP	k^m ϵ_{OH}^m (%)

^a Reaction rate constant taken from Calvert et al., 2002. ^b Kinetic isotope effects taken from Anderson et al., 2004. ^c Carbon isotope ratio of emissions taken from Rudolph et al. (2002) and Kornilova et al. (2016); for m-xylene the value reported for p+m-xylene is given. ^d Reaction occurs via OH abstraction (Atkinson et al., 1992) and the secondary carbon isotope effect is assumed to be negligible. ^e Rate constant from Grosjean (1991). ^f Estimated based on loss reaction proceeding mostly by addition to the aromatic ring (Grosjean, 1991) and the carbon kinetic isotope effects reported by Anderson et al. (2004). ^g Estimated on the assumption that reaction proceeds through primarily through addition pathway (Atkinson et al., 1980) and the kinetic isotope effect for reactions of aromatic VOC reported by Anderson et al. (2004). ^h Rate constant from Bejan et al. (2007). ⁱ Estimate based on the carbon kinetic isotope effects for reactions of aromatic VOC reported by Anderson et al. (2004). ^j Rate constant assumed to be the average of the rate constants for 3-me-2-NP ($3.69 \times 10^{-12} \text{ cm}^3 \text{ molec}^{-1} \text{ s}^{-1}$) and 4-me-2-NP reported by Bejan et al. (2007). ^k Rate constant estimated to be identical to the rate constant reported for 4-me-2-NP by Bejan et al. (2007). ^l Reaction rate constant from Atkinson and Aschmann (1990).

^m Assumed to have no loss reaction that results in carbon isotope fractionation, see text.

**Table 3.** Linear approximation for dependence of carbon isotope ratios and PCA for nitrophenols formed by the photochemical oxidation of aromatic VOC.

	R ²	Slope ^a (10 ⁻¹² % cm ³ s ⁻¹ molecules ⁻¹)	Intercept ^a (‰)	Limit δ ¹³ C ^b (‰)	Initial δ ¹³ C ^c (‰)
4-NP					
Scenario 2	0.993	4.28 (0.001)	-35.1 (0.002)	-28.1	-35.5
Scenario 3	0.967	14.4 (0.04)	-37.9 (0.005)	-34.8	-38.4
4-me-2-NP					
Scenario 2	0.985	64.7 (0.1)	-38.1 (0.004)	-32.5	-38.6
Scenario 3	0.985	64.7 (0.1)	-35.7 (0.005)	-30.1	-36.2
3-me-4-NP					
Scenario 2	0.982	80.7 (0.1)	-38.1 (0.005)	-33.1	-38.6
Scenario 3	0.982	80.9 (1.0)	-35.7 (0.006)	-30.7	-36.2
2-me-4-NP					
Scenario 2	0.988	56.4 (0.1)	-38.1 (0.003)	-32.0	-38.6
Scenario 3	0.988	56.6 (0.1)	-35.7 (0.004)	-29.6	-36.2
2,6-dime-4-NP					
Scenario 2	0.985	89.2 (0.1)	-36.2(0.004)	-30.3	-37.4
Scenario 3	0.985	89.4 (0.1)	-34.5 (0.07)	-28.5	-35.0

^a from linear regression for a range with <0.5 ‰ deviation from exact calculation; value in parenthesis is statistical error of linear regression. ^b Upper end of linear range where exact calculations deviate more than 0.5 ‰ from the linear approximation. ^c From exact calculations

Table 4. Averages and uncertainty of the mean PCA for nitrophenols in both PM and in the gas phase and PM calculated for Scenario 3. Also shown are the average carbon isotope ratios. The number of data points used is shown in brackets. For comparison PCA calculated from the carbon isotope ratios of the precursor VOC reported by Kornilova et al. (2016) for Toronto are included.

Precursor	Average PCA ^a (10 ¹¹ s molec cm ⁻³)	Product	Average δ ¹³ C (‰)	Average PCA (10 ¹¹ s molec cm ⁻³)
Benzene	3.1 ± 0.5 (43)	4-NP	-33.5 ± 0.3	4.7 ± 0.3 (58)
Toluene	0.85±0.11 (73)	Methyl- nitrophenols	-33.1±0.1	0.42±0.02 (120)
p,m- Xylene	0.34 ± 0.06 (56)	2,6-dime-4-NP	-33.4 ± 0.5	0.11 ± 0.04 (19)

^a Average carbon isotope ratio and PCA determined by Kornilova (2012) and Kornilova et al., (2016)



Table 5. Change of average PCA derived from carbon isotope ratios of nitrophenols resulting from changes in carbon isotope ratios of emissions and isotope fractionation for reactions of intermediates. The calculations were based on in Scenario 3.

Change	4-NP	4-me-2-NP	3-me-4-NP	2-me-4-NP	2,6-dime-4-NP
Δ PCA (10^{11} s molecules cm^{-3}) for decrease in source signature ($\delta^{13}\text{C}_0$) of 1 ‰	1.6	0.14	0.14	0.18	0.09
Resulting relative change (%)	34	35	28	36	45
Δ PCA (10^{11} s molecules cm^{-3}) for increase in fractionation for reaction of intermediates by 1 ‰	0.13	0.16	0.15	0.18	0.08
Resulting relative change (%)	3	25	36	32	52



Figure Captions

Figure 1. Proposed formation mechanism of 2-methyl-4-nitrophenol from toluene oxidation (adapted from Forstner et al., 1997).

Figure 2. Dependence between carbon isotope ratio and PCA ($\int[\text{OH}]dt$) for several nitrophenols calculated for different scenarios using a mechanistic model and mass balance. Also shown are the median, 10 and 90 percentiles as well as the lowest and highest carbon isotope ratios measured by Saccon et al. (2015) in an urban area. The triangles and squares represent the carbon isotope ratios of 3-methyl-4-nitrophenol and 2-methyl-4-nitrophenol, respectively, reported by Irei et al. (2015) for laboratory studies.

Figure 3. Dependence between carbon isotope ratio and PCA ($\int[\text{OH}]dt$) for 2-methyl-4-nitrophenol, its precursor (toluene) and the phenolic intermediate calculated for Scenario 3. Also shown are the median, 10 and 90 percentiles as well as the lowest and highest carbon isotope ratios for toluene reported by Kornilova et al. (2016) for an urban area in Toronto (Canada).

Figure 4. Frequency distribution of PCA determined from the carbon isotope ratios of 4-nitrophenol (a) and methylnitrophenols (b) using Scenario 3. For comparison the median (dotted line), 75 and 25 percentiles (dashed line) and 10 and 90 percentiles (solid line) determined by Kornilova et al. (2016) from carbon isotope ratios of benzene (a) and toluene (b) are included.

Figure 5. PCA distributions calculated for different depositional loss rates of 4-nitrophenol. The depositional loss rates are given as multiples of the chemical loss rate of 4-nitrophenol due to reaction with OH-radicals. For comparison, the PCA distribution determined from the precursor carbon isotope ratio distribution (Kornilova et al., 2016) is also shown (solid line).

Figure 6. Comparison of PCA distributions calculated for different depositional loss rates of 4-nitrophenol. The depositional loss rates are given as multiples of the chemical loss rate of 4-nitrophenol due to reaction with OH-radicals. For comparison, the PCA distribution determined from the 4-nitrophenol carbon isotope ratios reported by Saccon et al. (2015) are also shown. The error bars represent the statistical uncertainty resulting from the limited number of observations.

Figure 7. Average nitrophenol concentrations (a) and PCA (b) determined from carbon isotope ratios reported by Saccon et al. (2015) using Scenario 3 for different precipitation conditions during and before sampling. No rain: In total less than 1 mm on the day of sampling and the day before; light rain: between 1 mm and 10 mm precipitation on the day of sampling or a total of >4 mm on the day of sampling and the day before; heavy rain: > 20 mm precipitation on the day of sampling or > 10 mm on the day of sampling and > 20 mm on the day before. Precipitation data were taken from Environment Canada: Historical Data, Toronto North York site.

Figure 8. Plot of concentrations (black diamonds, left axis) and isotope ratios (open diamonds, right axis) of 2-methyl-4-nitrophenol as a function of the maximum wind speed during sampling (Environment Canada: Historical Weather Data, Toronto North York Site). Points were sorted in order of increasing wind speed and each point is an average of 10 filter samples; samples collected while there was precipitation were excluded. Error bars are the errors of the mean.



Figure 9. The PCA of 2-methyl-4-nitrophenol as a function of the maximum wind speed during sampling (Environment Canada: Historical Data, Toronto North York site). Points were sorted in order of increasing wind speed and each point is an average of 10 filter samples; samples collected while there was precipitation were excluded. Error bars are the errors of the mean.



Figures

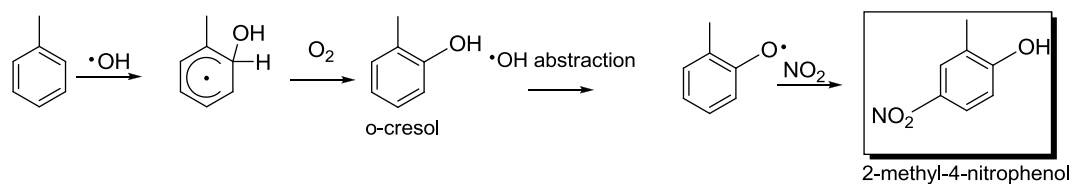
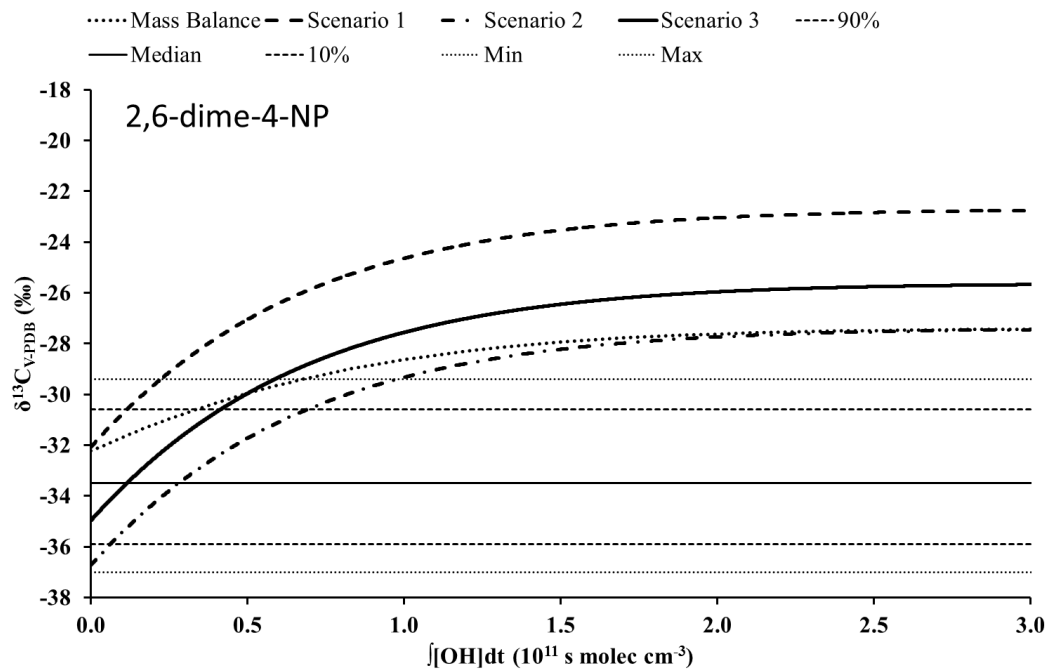


Figure 1. Proposed formation mechanism of 2-methyl-4-nitrophenol from toluene oxidation (adapted from Forstner et al., 1997).



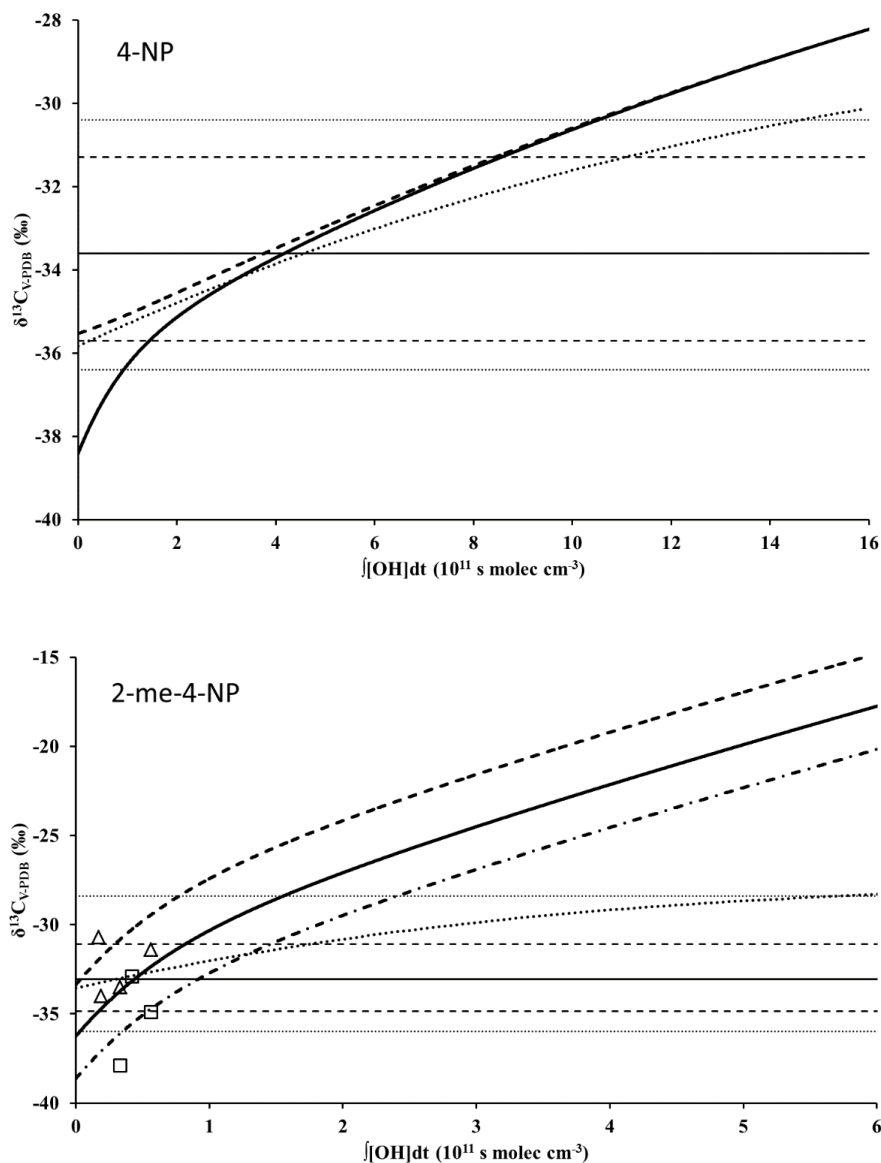


Figure 2. Dependence between carbon isotope ratio and PCA ($[\text{OH}]\text{dt}$) for several nitrophenols calculated for different scenarios using a mechanistic model and mass balance. Also shown are the median, 10 and 90 percentiles as well as the lowest and highest carbon isotope ratios measured by Saccon at al. (2015) in an urban area. The triangles and squares represent the carbon isotope ratios of 3-methyl-4-nitrophenol and 2-methyl-4-nitrophenol, respectively, reported by Irei et al. (2015) for laboratory studies.

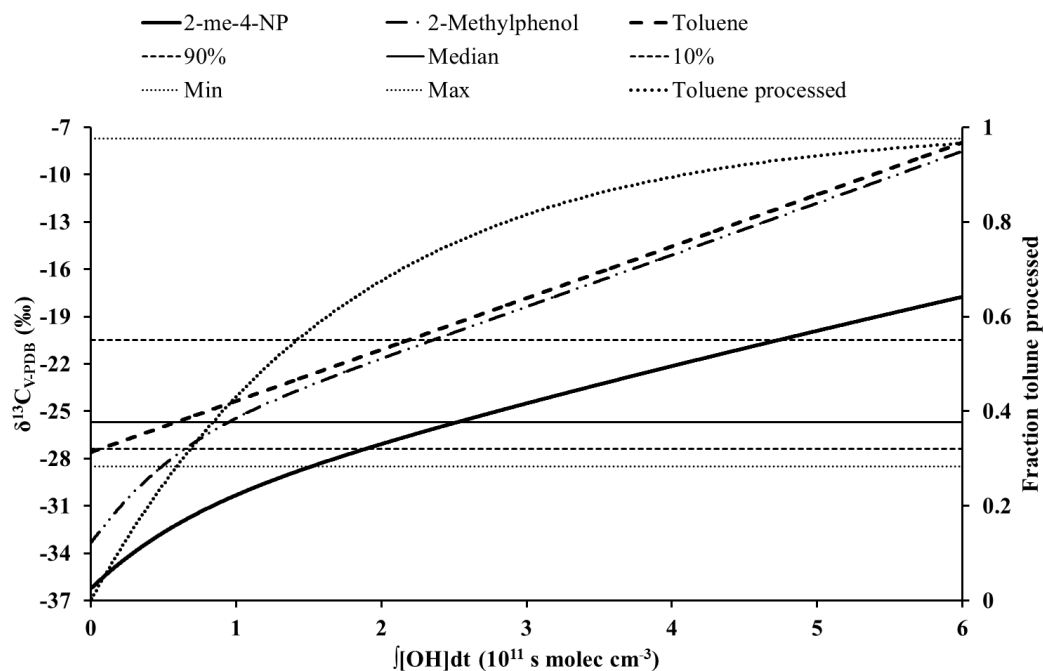


Figure 3. Dependence between carbon isotope ratio and PCA ($\int[\text{OH}]dt$) for 2-methyl-4-nitrophenol, its precursor (toluene) and the phenolic intermediate calculated for Scenario 3. Also shown are the median, 10 and 90 percentiles as well as the lowest and highest carbon isotope ratios for toluene reported by Kornilova et al. (2016) for an urban area in Toronto (Canada).

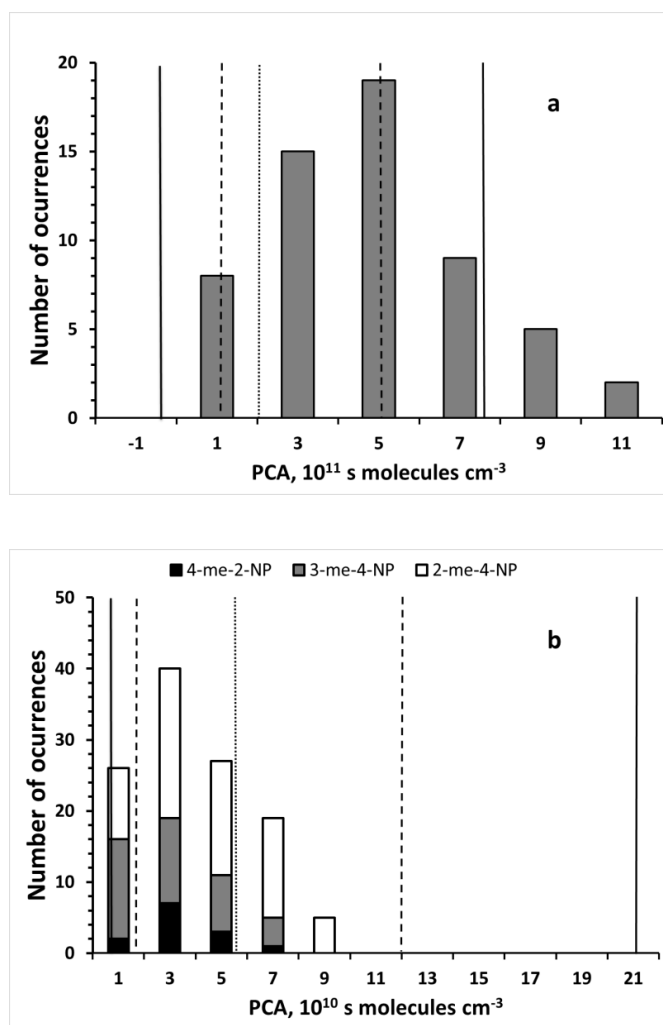


Figure 4. Frequency distribution of PCA determined from the carbon isotope ratios of 4-nitrophenol (a) and methylnitrophenols (b) using Scenario 3. For comparison the median (dotted line), 75 and 25 percentiles (dashed line) and 10 and 90 percentiles (solid line) determined by Kornilova et al. (2016) from carbon isotope ratios of benzene (a) and toluene (b) are included.

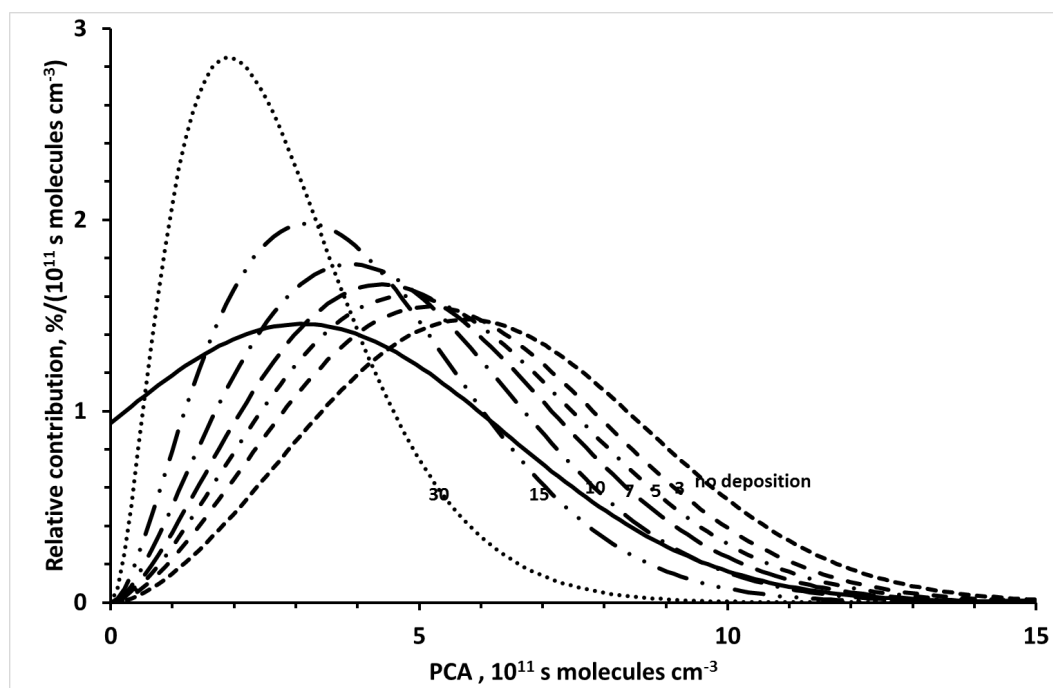


Figure 5. PCA distributions calculated for different depositional loss rates of 4-nitrophenol. The depositional loss rates are given as multiples of the chemical loss rate of 4-nitrophenol due to reaction with OH-radicals. For comparison, the PCA distribution determined from the precursor carbon isotope ratio distribution (Kornilova et al., 2016) is also shown (solid line).

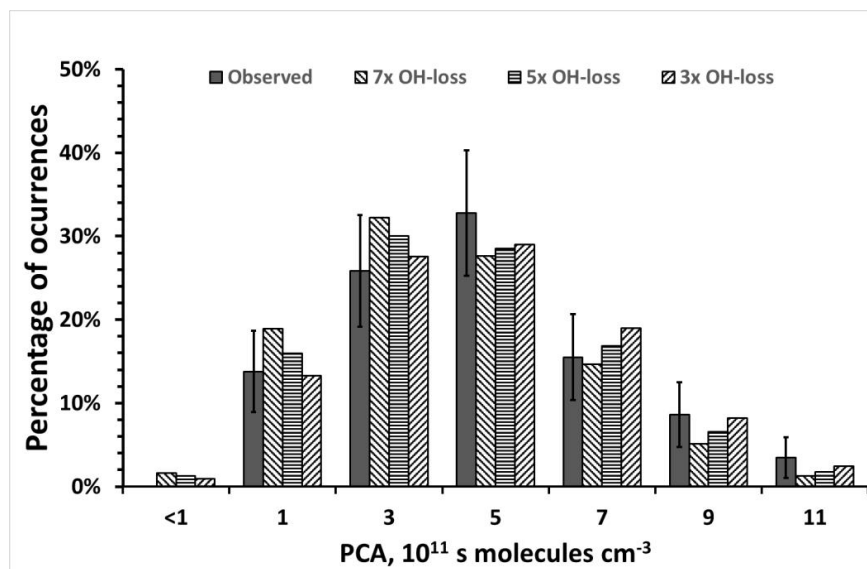


Figure 6. Comparison of PCA distributions calculated for different depositional loss rates of 4-nitrophenol. The depositional loss rates are given as multiples of the chemical loss rate of 4-nitrophenol due to reaction with OH-radicals. For comparison, the PCA distribution determined from the 4-nitrophenol carbon isotope ratios reported by Saccon et al. (2015) are also shown. The error bars represent the statistical uncertainty resulting from the limited number of observations.

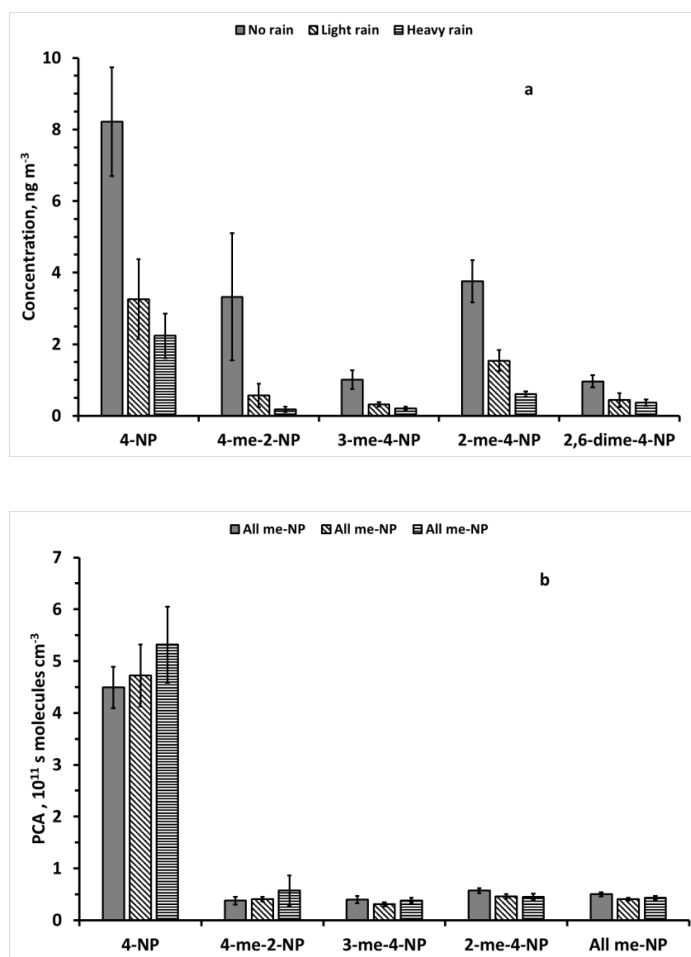


Figure 7. Average nitrophenol concentrations (a) and PCA (b) determined from carbon isotope ratios reported by Saccon et al. (2015) using Scenario 3 for different precipitation conditions during and before sampling. No rain: In total less than 1 mm on the day of sampling and the day before; light rain: between 1 mm and 10 mm precipitation on the day of sampling or a total of >4 mm on the day of sampling and the day before; heavy rain: > 20 mm precipitation on the day of sampling or > 10 mm on the day of sampling and > 20 mm on the day before. Precipitation data were taken from Environment Canada: Historical Data, Toronto North York site.

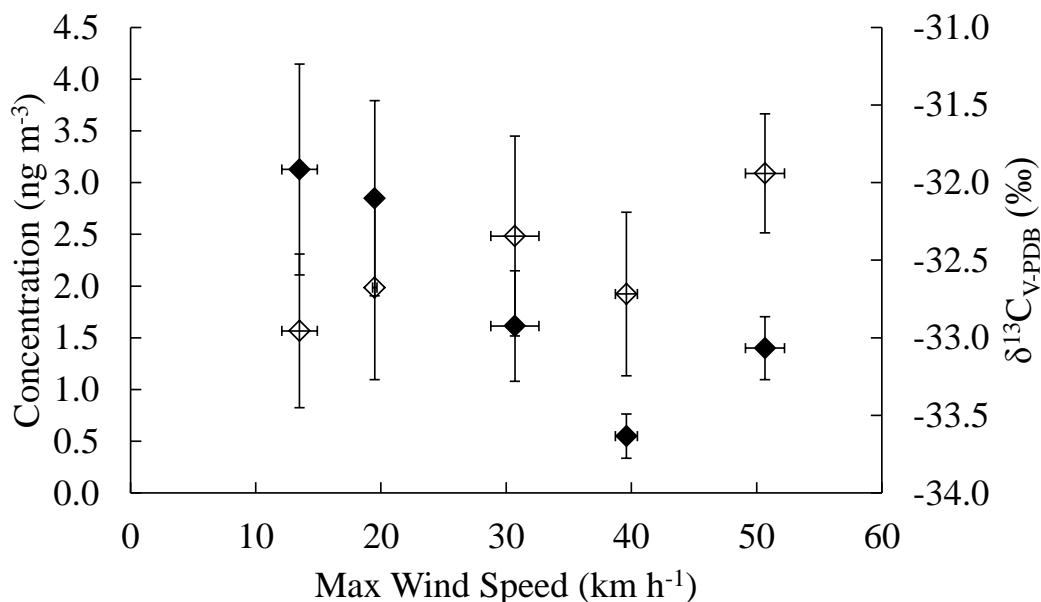


Figure 8. Plot of concentrations (black diamonds, left axis) and isotope ratios (open diamonds, right axis) of 2-methyl-4-nitrophenol as a function of the maximum wind speed during sampling (Environment Canada: Historical Weather Data, Toronto North York Site). Points were sorted in order of increasing wind speed and each point is an average of 10 filter samples; samples collected while there was precipitation were excluded. Error bars are the errors of the mean.

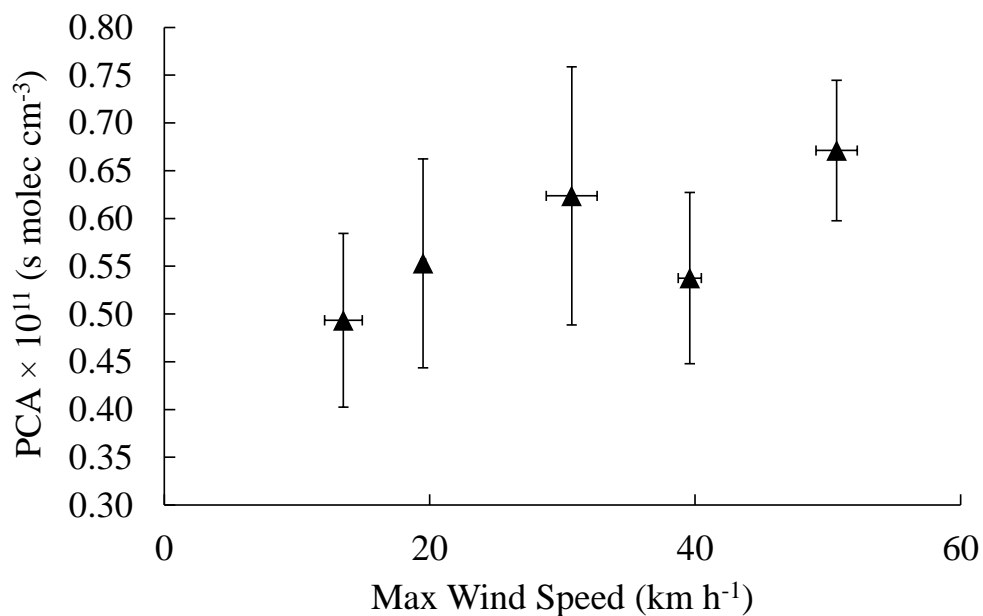


Figure 9. The PCA of 2-methyl-4-nitrophenol as a function of the maximum wind speed during sampling (Environment Canada: Historical Data, Toronto North York site). Points were sorted in order of increasing wind speed and each point is an average of 10 filter samples; samples collected while there was precipitation were excluded. Error bars are the errors of the mean.